OPTIMAL BEAMFORMING ON SYNTHETIC INTERFERENCE AND NOISE FOR ACTIVE PROCESSING OF MULTIPLET LINE ARRAYS

Sergey Simakov, Zhi Yong Zhang

Maritime Division
Defence Science and Technology Organisation
Edinburgh, Australia

Robert P. Goddard

Applied Physics Laboratory
University of Washington
Seattle, Washington, USA

ABSTRACT

Optimal beamforming on synthetic noise and interference is a flexible and intuitive technique for shaping beam patterns. In this method, suppression of arrivals from undesirable directions is achieved through introduction of synthetic interferences and optimal beamforming using the resulting noise-interference covariance matrix. We apply this approach to a general multiplet line array and test the algorithm on representative multi-channel time-series obtained for a quadruplet line array.

***Index Terms*—** multiplet line arrays, sonar simulation, optimal beamforming

1. INTRODUCTION

An optimal beamformer provides maximal array gain when the noise+interference covariance matrix is known or can be reliably estimated. In many practical situations of sonar signal processing, optimal beamformers obtained for one type of covariances are employed in cases with a rather different noise and interference structure. One immediate example is the conventional beamformer, which is an optimal beamformer obtained for a somewhat contrived case, when there are no interferences and the noise processes at different receiver elements are statistically identical and independent. We can adopt a similar approach and consider optimal beamforming on different forms of synthetic noise and interference in order to create beam patterns of desirable shapes.

Considering the narrow-band case, let $\tilde{\mathbf{x}}(t)$ be the complex envelope of the signal $\mathbf{x}(t)$ sampled at the receiver elements of the array ($\mathbf{x}(t) = \mathrm{Re}\{\tilde{\mathbf{x}}(t)e^{\mathrm{i}\omega t}\}$). There is a range of cases for which the noise component $\mathbf{R}_{\tilde{\mathbf{x}}:\mathrm{n}}$ of the combined noise+interference covariance matrix $\mathbf{R}_{\tilde{\mathbf{x}}:\mathrm{ni}} = \mathbf{R}_{\tilde{\mathbf{x}}:\mathrm{n}} + \mathbf{R}_{\tilde{\mathbf{x}}:\mathrm{i}}$ has an analytic form simple for calculation, isotropic noise is one example. The interference component $\mathbf{R}_{\tilde{\mathbf{x}}:\mathrm{i}}$ can also be readily calculated: if there are M independent interferences arriving from directions described by unit vectors $\boldsymbol{\nu}_m$ ($m = 1, \ldots, M$), then $\mathbf{R}_{\tilde{\mathbf{x}}:\mathrm{i}} = \sum_{m=1}^{M} 2\sigma_{\mathrm{i}:m}^2 \mathbf{v}(\boldsymbol{\nu}_m)\mathbf{v}^{\mathrm{H}}(\boldsymbol{\nu}_m)$,where $\sigma_{\mathrm{i}:m}^2$ is the power of the narrow-band interference process m at the center of the array and $\mathbf{v}(\boldsymbol{\nu})$ is the array manifold vector for the look direction $\boldsymbol{\nu}$ and the center frequency ω.

By appropriately selecting $\{\boldsymbol{\nu}_m;\, \sigma_m^2\}$, one can devise covariance matrix $\mathbf{R}_{\tilde{\mathbf{x}}:\mathrm{ni}}$ and use it in the optimal beamformer in order to build beam patterns in which arrivals from undesirable directions are suppressed.

In this work we use optimal beamforming on synthetic interferences in order to shape beam patterns for a multiplet line array. One of the tasks commonly considered in beamforming of multiplet line arrays is elimination of port/starboard ambiguity [1]. Similarly to [1] we employ beamspace processing [2, 3] in which preliminary beams are obtained by conventionally beamforming line sub-arrays. We focus on an active narrow-band case.

The derivation of the beamformer is provided in section 2. In section 3 we describe generation of representative multichannel time series for testing the beamformer and discuss the processing steps and the outputs.

2. DERIVATION OF THE BEAMFORMER

Consider a multiplet line array consisting of K multiplets each of which comprising of L receiver elements (see Fig. 1). Such arrays can be viewed as a combination of L line sub-arrays, so they are also referred to as multi-line arrays [4].

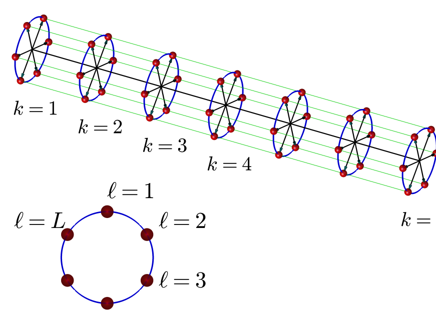

Fig. 1. Schematic of a multiplet line array. The multiplet's diameter is assumed to be small compared to the spacing between them.

The derivation below is applicable to more general arrays than shown in Fig. 1. In particular, it covers the case of mildly twisted and bent multi-line arrays, and, upon minor modifications, the method can also be used when some of the array elements are removed.

Multi-channel signals received by array elements can be represented as a column vector $\mathbf{x}(t)$ of real time dependent functions $x_s(t)$, where s is the consecutive number of the receiver element ($s = 1, \ldots, K \times L$). Index s can be referred to as the global index. The discrete time-series data can be formed into an N-by-$K \times L$ array, where N is the number of sampling times.

Considering active narrow-band case, let ω be the center frequency and $\tilde{\mathbf{x}}(t)$ be the complex envelope of $\mathbf{x}(t)$. For look direction $\boldsymbol{\nu}$, define time delays using the dot product

$$\tau_s(\boldsymbol{\nu}) \equiv (\mathbf{d}_s \cdot \boldsymbol{\nu})/c \tag{1}$$

where $\mathbf{d}_s$ is the radius-vector of array element s and c is the speed of sound. Let $s = \mu(k, \ell)$ be the global index corresponding to element ℓ in multiplet k. In our enumeration of array elements, we have $\mu(k, \ell) = L \times (k-1) + \ell$. Elements $\mu(k, \ell)$ ($k = 1, \ldots, K$) form line sub-array ℓ. Let $v_{k,\ell}(\boldsymbol{\nu}) = e^{\mathrm{i}\omega\tau_{\mu(k,\ell)}(\boldsymbol{\nu})}$, then the array manifold vector of sub-array ℓ is

$$\mathbf{v}_\ell(\boldsymbol{\nu}) \equiv \begin{bmatrix} v_{1,\ell}(\boldsymbol{\nu}) \\ \vdots \\ v_{K,\ell}(\boldsymbol{\nu}) \end{bmatrix} \qquad (\ell = 1, \ldots, L). \tag{2}$$

For a given look direction $\boldsymbol{\nu}_0$ obtain time-shifted complex envelopes

$$\tilde{x}_{k,\ell}(t) \equiv \tilde{x}_{\mu(k,\ell)}(t - \tau_{\mu(k,\ell)}(\boldsymbol{\nu}_0)) , \tag{3}$$

where $k = 1, \ldots, K$ and $\ell = 1, \ldots, L$, and form vectors

$$\tilde{\mathbf{x}}_\ell(t) \equiv \begin{bmatrix} \tilde{x}_{1,\ell}(t) \\ \vdots \\ \tilde{x}_{K,\ell}(t) \end{bmatrix} , \qquad \ell = 1, \ldots, L. \tag{4}$$

Conventionally beamform each of the sub-arrays and combine the outputs into a single vector

$$\tilde{\mathbf{z}}(t) \equiv \begin{bmatrix} \mathbf{v}_1^{\mathrm{H}}(\boldsymbol{\nu}_0)\tilde{\mathbf{x}}_1(t) \\ \vdots \\ \mathbf{v}_L^{\mathrm{H}}(\boldsymbol{\nu}_0)\tilde{\mathbf{x}}_L(t) \end{bmatrix} \tag{5}$$

The array output is

$$\tilde{y}(t) = \mathbf{h}^{\mathrm{H}}\tilde{\mathbf{z}}(t) . \tag{6}$$

The associated real signal is $y(t) = \mathrm{Re}\left\{\tilde{y}(t)e^{\mathrm{i}\omega t}\right\}$. We will cross-correlate (6) against the complex envelope of the replica of the transmitted pulse.

The coefficients $\mathbf{h}$ used in (6) are obtained by postulating a special synthetic form of noise and interference and maximising the array gain

$$G \equiv \frac{\mathcal{E}/P_{y:\mathrm{ni}}}{\mathcal{E}_0/\sigma^2_{\mathrm{ni}}} . \tag{7}$$

Equation (7) uses the following notation.

- $\mathcal{E}_0$ is the energy of the echo received at each receiver element. For the considered frequencies, we have

$$\mathcal{E}_0 \equiv \int_{t_0}^{t_0+T} [x_{k,\ell}(t)]^2 dt \approx \frac{1}{2}\int_{t_0}^{t_0+T} |\tilde{x}_{k,\ell}(t)|^2 dt$$

where t_0 is the time of arrival of the echo at the center of the array, T is pulse length, and in this calculation we consider only echo arrivals. In the derivation of the beamformer we assume single-path straight-line propagation, so the resulting idealised echo can be described near the array by a function of the form $Q(t - r/c)/r_0$, where r is the distance from the target and r_0 is the distance between the target and the center of the array. If $\tilde{Q}(t)$ is the complex envelope of $Q(t)$, we obtain

$$\mathcal{E}_0 \approx \frac{1}{2r_0^2}\int_0^T |\tilde{Q}(t)|^2 dt \tag{8}$$

- σ^2_{ni} is the combined power of the noise and interference processes at each receiver element – we assume that these stationary processes are independent, so

$$\sigma^2_{\mathrm{ni}} = \sigma^2_{\mathrm{i}} + \sigma^2_{\mathrm{n}}, \tag{9}$$

where σ^2_{i} and σ^2_{n} are the powers of the interference and noise respectively.

- $\mathcal{E}$ is the energy of the echo-only output of the array, i.e.

$$\mathcal{E} \equiv \int_{t_0}^{t_0+T} [y(t)]^2 dt \approx \frac{1}{2}\int_{t_0}^{t_0+T} |\tilde{y}(t)|^2 dt .$$

Use (6) and (8) to obtain

$$\begin{aligned} \mathcal{E} &= \left[\frac{K^2}{2r_0^2}\int_0^T |\tilde{Q}(t)|^2 dt\right] \mathbf{h}^{\mathrm{H}}\mathbf{u}(\boldsymbol{\nu}_0, \boldsymbol{\nu}_0)\mathbf{u}^{\mathrm{H}}(\boldsymbol{\nu}_0, \boldsymbol{\nu}_0)\mathbf{h} \\ &= \mathcal{E}_0 K^2 |\mathbf{h}^{\mathrm{H}}\mathbf{u}_0|^2 \end{aligned} \tag{10}$$

where

$$\mathbf{u}(\boldsymbol{\nu}_a, \boldsymbol{\nu}_b) \equiv \frac{1}{K}\begin{bmatrix} \mathbf{v}_1^{\mathrm{H}}(\boldsymbol{\nu}_a)\mathbf{v}_1(\boldsymbol{\nu}_b) \\ \vdots \\ \mathbf{v}_L^{\mathrm{H}}(\boldsymbol{\nu}_a)\mathbf{v}_L(\boldsymbol{\nu}_b) \end{bmatrix} \tag{11}$$

and

$$\mathbf{u}_0 \equiv \mathbf{u}(\boldsymbol{\nu}_0, \boldsymbol{\nu}_0) = \begin{bmatrix} 1 \\ \vdots \\ 1 \end{bmatrix} . \tag{12}$$

- $P_{y:\mathrm{ni}}$ is the power of the array output when only noise and interference are present, i.e. $y(t) = y_{\mathrm{ni}}(t)$:

$$P_{y:\mathrm{ni}} = \mathrm{E}\left[|y_{\mathrm{ni}}(t)|^2\right] = \frac{1}{2}\mathbf{h}^{\mathrm{H}}\mathbf{R}_{\tilde{\mathbf{z}}:\mathrm{ni}}\mathbf{h}, \tag{13}$$

where $\mathbf{R}_{\tilde{\mathbf{z}}:\mathrm{ni}}$ is the covariance matrix of the associated $\tilde{\mathbf{z}}(t)$ (and we also use similar notation $\mathbf{R}_{\tilde{\mathbf{z}}:\mathrm{n}}$ and $\mathbf{R}_{\tilde{\mathbf{z}}:\mathrm{i}}$ for *noise*- and *interference*-only processes). From independence of noise and interference processes we obtain $\mathbf{R}_{\tilde{\mathbf{z}}:\mathrm{ni}} = \mathbf{R}_{\tilde{\mathbf{z}}:\mathrm{i}} + \mathbf{R}_{\tilde{\mathbf{z}}:\mathrm{n}}$.

The complex envelope covariance matrix $\mathbf{R}_{\tilde{\mathbf{z}}:\mathrm{i}}$ of an interference arriving from direction $\boldsymbol{\nu}_{\mathrm{i}}$ is (*cf.* equation (10))

$$\mathbf{R}_{\tilde{\mathbf{z}}:\mathrm{i}} = 2\sigma_{\mathrm{i}}^2 K^2 \mathbf{u}(\boldsymbol{\nu}_0, \boldsymbol{\nu}_{\mathrm{i}})\mathbf{u}^{\mathrm{H}}(\boldsymbol{\nu}_0, \boldsymbol{\nu}_{\mathrm{i}}) \tag{14}$$

Let $\tilde{n}_{k,\ell}(t)$ be the reduction of $\tilde{x}_{k,\ell}(t)$ to noise-only component. In the development of the beamformer we postulate that each $\tilde{n}_{k,\ell}(t)$ results from a synthetic isotropic noise obtained as a limiting case of a multitude of independent isotropically distributed equal interferences arriving at the array. We assume that variations of $\tilde{n}_{k,\ell}(t)$ within time intervals of length $\max_s(|\mathbf{d}_s|/c)$ are insignificant and can be ignored. If $\tilde{n}_A(t)$ and $\tilde{n}_B(t)$ were obtained for points A and B, then we would have

$$\mathrm{E}\left[\tilde{n}_A(t)\tilde{n}_B^*(t)\right] = 2\sigma_{\mathrm{n}}^2 \rho(D_{AB}, \omega), \tag{15}$$

where $\rho(D, \omega) = \mathrm{sinc}(D\omega/c)$, D_{AB} is the distance between the points A and B, and $\mathrm{sinc}(\cdot)$ is an unnormalised sinc function. Assuming that the distance between the multiplets is large enough ($> \pi c/\omega$), we can ignore the correlation between the noise processes at receiver elements of different multiplets:

$$\mathrm{E}\left[\tilde{n}_{k,\ell}(t)\tilde{n}_{q,p}^*(t)\right] \simeq 0 \qquad (k \neq q)\,. \tag{16}$$

Because the size of the multiplet is small, the noise correlation between elements within a multiplet cannot be ignored, so by (15) we have

$$\mathrm{E}\left[\tilde{n}_{k,\ell}(t)\tilde{n}_{k,p}^*(t)\right] = 2\sigma_{\mathrm{n}}^2 \rho(d_{\ell p}, \omega), \tag{17}$$

where $d_{\ell p}$ is the distance between elements ℓ and p within a multiplet. Calculate elements of the covariance matrix $\mathbf{R}_{\tilde{\mathbf{z}}:\mathrm{n}}$:

$$\begin{aligned} [\mathbf{R}_{\tilde{\mathbf{z}}:\mathrm{n}}]_{\ell p} &= \mathrm{E}\left[\sum_{k=1}^{K} v_{k,\ell}^*(\boldsymbol{\nu}_0)\tilde{n}_{k,\ell}(t) \sum_{q=1}^{K} v_{q,p}(\boldsymbol{\nu}_0)\tilde{n}_{q,p}^*(t)\right] \\ &= 2\sigma_{\mathrm{n}}^2 \rho(d_{\ell p}, \omega)\mathbf{v}_\ell^{\mathrm{H}}(\boldsymbol{\nu}_0)\mathbf{v}_p(\boldsymbol{\nu}_0)\,. \end{aligned} \tag{18}$$

Substitute (9), (10) and (13) into (7) to obtain

$$G = 2K^2(\sigma_{\mathrm{i}}^2 + \sigma_{\mathrm{n}}^2)\frac{|\mathbf{h}^{\mathrm{H}}\mathbf{u}_0|^2}{\mathbf{h}^{\mathrm{H}}\mathbf{R}_{\tilde{\mathbf{z}}:\mathrm{ni}}\mathbf{h}} \tag{19}$$

A standard procedure based on the substitution $\mathbf{w} = \mathbf{R}_{\tilde{\mathbf{z}}:\mathrm{ni}}^{1/2}\mathbf{h}$ and application of the Cauchy-Schwarz inequality gives (e.g. [5], [6, ch.5], or [7, ch.10])

$$\mathbf{h}_{\max} \equiv \operatorname{argmax} G(\mathbf{h}) = \gamma \mathbf{R}_{\tilde{\mathbf{z}}:\mathrm{ni}}^{-1}\mathbf{u}_0\,,$$

where γ is an arbitrary non-zero number which we set to 1.

By (14), $\mathbf{R}_{\tilde{\mathbf{z}}:\mathrm{ni}} = \mathbf{R}_{\tilde{\mathbf{z}}:\mathrm{ni}}(\boldsymbol{\nu}_0, \boldsymbol{\nu}_{\mathrm{i}})$. The obtained beamformer automatically suppresses arrivals from the direction $\boldsymbol{\nu}_{\mathrm{i}}$. To suppress the ambiguity present in conventionally beamformed line arrays we select vector $\boldsymbol{\nu}_{\mathrm{i}}$ by pointing it in the direction symmetric to $\boldsymbol{\nu}_0$ with respect to the array axis:

$$\boldsymbol{\nu}_{\mathrm{i}} = \boldsymbol{\nu}_{\mathrm{i}}(\boldsymbol{\nu}_0) = \boldsymbol{\nu}_0 - 2(\boldsymbol{\nu}_0 \cdot \mathbf{e}_y)\mathbf{e}_y\,, \tag{20}$$

where $\mathbf{e}_y$ is the unit vector pointing in the starboard direction of the array.

Thus, the obtained beamformer coefficients for (6) are

$$\mathbf{h}_{\max} = \mathbf{h}(\boldsymbol{\nu}_0) = \mathbf{R}_{\tilde{\mathbf{z}}:\mathrm{ni}}^{-1}(\boldsymbol{\nu}_0)\mathbf{u}_0 \tag{21}$$

where $\mathbf{R}_{\tilde{\mathbf{z}}:\mathrm{ni}}(\boldsymbol{\nu}_0) = \mathbf{R}_{\tilde{\mathbf{z}}:\mathrm{ni}}(\boldsymbol{\nu}_0, \boldsymbol{\nu}_{\mathrm{i}}(\boldsymbol{\nu}_0))$.

3. TESTING THE BEAMFORMER

3.1. Generating representative multi-channel time series

We tested the optimal beamformer using simulated multi-channel signals generated by the Sonar Simulation Toolset (SST) [8] software. Artificial time series produced by the SST have a good degree of realism and statistical accuracy. The SST is capable of simulating very complex scenarios which span far beyond the simple single-path straight-line propagation assumptions used in the derivation of the beamformer. For our tests we chose a simple case with a nearly constant ocean depth of approximately 1950 m and a sound speed profile resulting in surface duct propagation. An omni-directional transmitter was used with a linear FM sweep with center frequency 1850 Hz, bandwidth 100 Hz, and source level 210 dB (re $\mu\mathrm{Pa}^2$ at 1 m). The duration of the ping was 0.5 sec and the time interval between the pings was 40 sec. The receiver constituted a line of 31 quadruplets ($L = 4$, $K = 31$) located 70 m behind the transmitter. The spacing between multiplets was 0.4 m (0.5 wavelength), and the radius of each multiplet is 0.05 m (0.0625 wavelength). Both receiver and transmitter were towed in line at a 50 m depth. For easier interpretation, the tow ship was nearly stationary slowly moving to the North. The target commenced at a range of approximately 11.7 km from the source and 45 degrees forward of broadside moving to the North West with the speed of 5.5 knots (see Fig. 3). The target was modelled as a single point scatterer with target strength of 10 dB re m^2. Reverberation is due to surface waves from a wind speed of 4.5 m/s. Ambient isotropic noise was included at 40 dB re $\mu\mathrm{Pa}^2/Hz$ and constant in the band. Tow ship interference was modelled as an omni-directional source emitting a broadband noise with a spectral level of 126 dB re $\mu\mathrm{Pa}^2/Hz$ at 1 m in the band. We chose complex envelope representation for SST's output, with sample rate 1 kHz and center frequency 1850 Hz.

3.2. Processing steps and outputs

The key processing steps were based on derivation steps of Section 2.

1. Filter and extract complex envelopes from multi-channel time series
2. For a given look direction $\boldsymbol{\nu}_0$:
   (a) Obtain $\tilde{\mathbf{z}}(t)$ by conventionally beamforming each of the singlet line arrays comprising the multiplet line array (see equation (5)).

(b) Select σ_{i} and σ_{n} for the synthetic interference and noise. Use (21) to obtain $\mathbf{h}(\boldsymbol{\nu}_0)$, then substitute into (6) and obtain $\tilde{y}(t)$.

(c) Cross-correlate $\tilde{y}(t)$ with the complex envelope of the replica and take the absolute value.

(d) Normalise the result to suppress the reverberation.

Synthetic interference in Step 2 (b) is used to eliminate the port/starboard ambiguity present in conventional line arrays. The synthetic noise is required to regularise the inversion of $\mathbf{R}_{\tilde{\mathbf{z}}:\mathrm{ni}}$: since $\operatorname{rank} \mathbf{u}(\boldsymbol{\nu}_0, \boldsymbol{\nu}_{\mathrm{i}}) = 1$, the covariance matrix $\mathbf{R}_{\tilde{\mathbf{z}}:\mathrm{ni}}$ becomes singular if σ_{n} is zero.

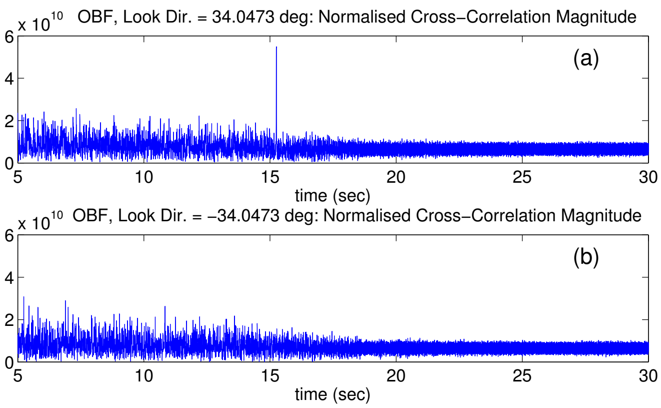

Fig. 2. Outputs of the optimal beamformer: normalised cross-correlation magnitude.

Time series data generated for a quadruplet line array were used to verify the port/starboard ambiguity elimination step. The results in Figure 2 demonstrate that the method does remove the ambiguity: plots in Figure 2 (a) were obtained for the steering direction pointing at the target, while plots in Figure 2 (b) were obtained for a steering vector symmetric with respect to the axis of the array.

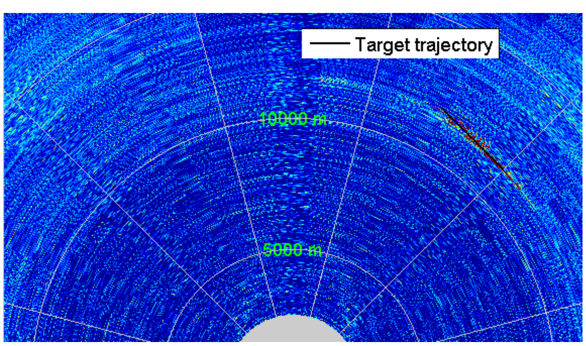

Fig. 3. A Plan Position Indicator (PPI) display of 30-ping beamforming history for a simulated example.

Plots in Figure 2 display two scans for a single ping from a 30-ping simulation. A PPI display of the entire beamforming history obtained in this simulation is provided in Figure 3.

Results in Fig. 2 and 3 can be further illustrated by examination of power patterns of the obtained beams. The array power pattern $\mathrm{PP}(\boldsymbol{\nu}, \boldsymbol{\nu}_0)$ is obtained by fixing the steering direction $\boldsymbol{\nu}_0$ and considering the power ratio

$$\mathrm{PP}(\boldsymbol{\nu}, \boldsymbol{\nu}_0) = \frac{P_{y:\mathrm{i}}(\boldsymbol{\nu}_0, \boldsymbol{\nu})}{P_{y:\mathrm{i}}(\boldsymbol{\nu}_0, \boldsymbol{\nu}_0)} = \frac{|\mathbf{h}^{\mathrm{H}}(\boldsymbol{\nu}_0)\mathbf{u}(\boldsymbol{\nu}_0, \boldsymbol{\nu})|^2}{|\mathbf{h}^{\mathrm{H}}(\boldsymbol{\nu}_0)\mathbf{u}_0|^2} \tag{22}$$

for different test directions $\boldsymbol{\nu}$.

Figures 4 (a) and (b) show beam patterns of the optimal and conventional beamformers obtained for the steering direction considered in Figures 2. The optimal power pattern in Figure 4 (a) shows that the arrivals from the ambiguous direction are suppressed.

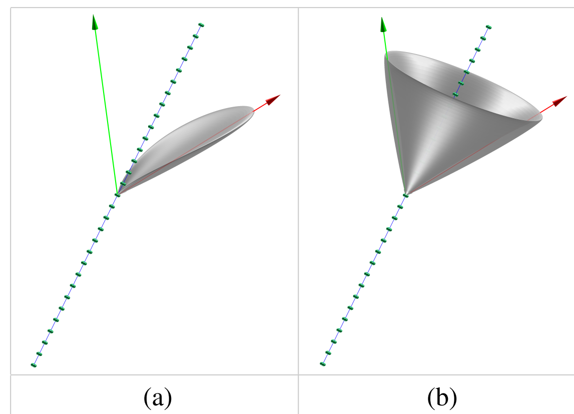

Fig. 4. Array power patterns at the center frequency (1850 Hz): (a) optimal beamformer, and (b) conventional beamformer. The red arrow points in the steering direction, while the green arrow points in the ambiguous direction.

4. CONCLUSION

In this work we considered application of optimal beamforming to active processing of multiplet line arrays. In our method the beamforming coefficients are obtained using a covariance matrix corresponding to appropriately chosen synthetic quasi-interference and isotropic noise. Examination of array power patterns and processing outputs shows that the resulting beamformer is free from the port/starboard ambiguity present in the conventionally beamformed line arrays. The beamformer has been tested on representative multi-channel time series generated using the Sonar Simulation Toolset (SST).

5. ACKNOWLEDGEMENTS

SST was created by a team led by Robert Goddard at the Applied Physics Laboratory, University of Washington (APL-UW), Seattle, WA USA, funded primarily by the US Office of Naval Research (ONR). It was provided to DSTO through The Technical Cooperation Program (TTCP) [9].

6. REFERENCES

[1] J. Groen, S. P. Beerens, R. Been, Y. Doisy, and E. Noutary, "Adaptive port-starboard beamforming of triplet sonar arrays," *Oceanic Engineering, IEEE Journal of*, vol. 30, no. 2, pp. 348–359, April 2005.

[2] D. A. Gray, "Formulation of the maximum signal-to-noise ratio array processor in beam space," *The Journal of the Acoustical Society of America*, vol. 72, no. 4, pp. 1195–1201, 1982.

[3] H. L. Van Trees, *Optimum Array Processing: Detection, Estimation, and Modulation Theory*, Detection, Estimation, and Modulation Theory. Wiley, 2002.

[4] R. P. Hodges, *Underwater Acoustics: Analysis, Design and Performance of Sonar*, Wiley, 2010.

[5] H. Cox, "Resolving power and sensitivity to mismatch of optimum array processors," *The Journal of the Acoustical Society of America*, vol. 54, no. 3, pp. 771–785, 1973.

[6] P. Stoica and R.L. Moses, *Spectral Analysis of Signals*, Pearson Prentice Hall, 2005.

[7] F. B. Jensen, W. A. Kuperman, M. B. Porter, and H. Schmidt, *Computational Ocean Acoustics*, Springer, second edition, 2011.

[8] R. P. Goddard, "The sonar simulation toolset, release 4.6: Science, mathematics, and algorithms," Tech. Rep. APL-UW TR 0702, Applied Physics Laboratory, University of Washington, Seattle, WA, October 2008.

[9] "The Technical Cooperation Program," Available at: http://www.dtic.mil/ttcp/.